

Simulation of Cr(VI) Removal in a Biofilm Reactor System and Optimisation Using an Ecological Algorithm

Evans M. N. Chirwa^{a,*}, Pulane E Molokwane^b, Hendrik G. Brink^a, Yi-Tin Wang^c

^aWater Utilisation and Environmental Engineering Division, Department of Chemical Engineering, University of Pretoria

^bOloenviron (Pty) Ltd, Centurion, Pretoria, South Africa

^cDepartment of Civil Engineering, University of Kentucky, Lexington Ky, 40506, United States of America

evans.chirwa@up.ac.za

A one-dimensional diffusion-reaction model was developed to simulate the removal of the carcinogenic transitional metal, Cr(VI), in a biofilm reactor with glucose and phenolic compounds as sole supplied carbon and energy sources in different runs. Substrate utilization and Cr(VI) reduction in the biofilm was best represented by a system of (second-order) partial differential equations (PDEs). Organic acid metabolic intermediates were measured and included in the dynamic model. The PDE system was solved by the (fourth-order) Runge-Kutta method adjusted for mass transport resistance using the (second-order) Crank-Nicholson and Backward Euler finite difference methods. A heuristic procedure, genetic search algorithm (GSA), was used to find global optimum values of Cr(VI) reduction and substrate utilization rate kinetic parameters. The fixed-film bioreactor system yielded higher values of the maximum specific Cr(VI) reduction rate coefficient and Cr(VI) reduction capacity ($k_{mc} = 0.062$ 1/h, and $R_c = 0.13$ mg/mg, respectively) than previously determined in batch reactors ($k_{mc} = 0.022$ 1/h and $R_c = 0.012$ mg/mg). The model predicted effluent Cr(VI) concentration with 98.9% confidence ($\sigma_y^2 = 2.37$ mg²/L², $N = 119$) and effluent glucose and phenol concentration with 96.4% and 99.3% confidence ($\sigma_{y(w)}^2 = 5402$ mg²/L², $N = 121$, $w = 100$) over a wide range of Cr(VI) loadings (10–500 mg Cr(VI)/L/d).

1. Introduction

Cr(VI) exists in the environment in the form of divalent oxyanions (chromate, CrO₄²⁻, and dichromate, Cr₂O₇²⁻). Chromate and dichromate oxyanions are highly mobile carcinogenic hexavalent forms of chromium (WHO, 1975). Cr(VI) pollution can be remediated by consortia or mixed cultures of Cr(VI) reducing organisms working together in synergy (Molokwane and Chirwa, 2010). This project aimed at safely removing Cr(VI) from polluted water using fixed-film, packed-bed biofilm reactors. Diffusion of Cr(VI) in the aquatic phase was described by the Nernst-Planck/Poisson laws wherein electroneutrality in the system is preserved by the coupling of transport of all charged diffusing species in solution (Dreyer et al., 2020). The Cr(VI) diffusion coefficient (D_{cw}) was estimated using the *Nernst-Haskell* ion diffusion theory for dilute ionic solutions (Eq. 1) (Samson et al., 2003).

$$D_{cw} = \frac{RT}{F^2} \cdot \frac{\lambda}{\gamma_i} \quad (1)$$

Mass transport coefficients of species i (k_{Li}) were correlated to the Reynolds number (Re) and Schmidt number (Sc) by the *Frössling correlation* (Frössling, 1938) (Eqs. 2-3):

$$k_{Li} = \frac{D_{iw}}{L_{iw}} = 0.6 \cdot \left(\frac{D_{iw}}{d_p} \right) \text{Re}^{1/2} \cdot \text{Sc}^{1/3} \quad (2)$$

$$k_{Li} = 0.6 \cdot \left(\frac{D_{iw}^{2/3}}{\nu^{1/6}} \right) \cdot \left(\frac{u^{1/2}}{d_p^{1/2}} \right) \quad (3)$$

, where u = bulk liquid velocity (LT^{-1}), d_p = diameter of glass beads (L), ν = kinematic viscosity (LT^{-1}), and D_{iw} = diffusion coefficient (L^2T^{-1}) of species i in water, and L_w = stagnant liquid layer thickness (L). The Reynolds number is a function of bulk liquid velocity u and packing material particle size d_p , $Re = u \cdot d_p/\nu$, and Schmidt numbers is given as a constant, $Sc = \nu/D_{iw}$, such that the mass transfer coefficient k_{Li} (LT^{-1}) is only a function of u and d_p under constant temperature. In this study, the propagation of effluent pollutant and substrate concentration profiles was generated using a (fourth-order) Runge-Kutta method adjusted for mass transport resistance using the (second-order) Crank-Nicholson and Backward Euler finite difference solution.

Traditional ways of multi-system evaluation involving several non-linear systems have been previously simplified due to limitations in computational resources. With increased availability of computational speed and storage, it is now possible to utilise machine learning and evolutionally computational theory to achieve better results (Jaluague, 2023).

In this study, a heuristic algorithm, Genetic Search Algorithm (GSA), was used to find global optimum values of Cr(VI) reduction and substrate utilization rate kinetic parameters following principles derived in genetic algorithms (Tsai et al., 1996) and orthogonal arrays from the Taguchi Method (Sendin et al., 2004). The model successfully predicted the operation of a laboratory-scale fixed-film bioreactor with agreeable trends for Cr(VI) and organic substrate concentration for a period of 700 days.

2. Experimental Methods

2.1 Reactor Setup and Operational Conditions

The reactor column was constructed from a 20 cm long by 3.8 cm internal diameter Pyrex glass column (Corning Glassware Co., Corning, NY) packed with 11,101 (3mm diameter) spherical Pyrex (Corning Co.) glass beads (Fig. 1). The entire packed-bed bioreactor had a total surface area of 3140 cm² and a clean-bed pore volume, $V_B = 104.7$ mL. To start-up the reactor, a 100 mL coculture of *P. putida* (6×10^{10} cells) and *E. coli* (3.5×10^{10} cells) was charged directly into a port at the bottom of the reactor. The reactor was then operated under an influent phenol concentration of 350 mg/L and 24 hours HRT until a biofilm was observed on the glass beads after 10 days of operation. Different influent phenol concentrations of 500, 800, 1000, 1300 mg/L were tested, for 5 days at each concentration, to determine optimum phenol loading for the experiment. Phenol was detected in the effluent when the reactor was operated at influent phenol concentrations of 1000 and 1300 mg/L. An influent phenol concentration of 800 mg/L was thus chosen for the rest of the experiment. Biofilm formation was observed under an Olympus microscope (Model BH-2, Rocky Mountain Microscope Corp., Ft. Collins, CO) on sampled glass beads after 30 days of operation.

2.2 Biofilm Reactor Theoretical Basis

Biofilm mass balance equations were coupled to the reaction rate terms based on the biofilm mass conservation and continuum principles previously derived by Wanner and Gujer (1986). The mass balances of dissolved species and biomass across an infinitesimal biofilm section (δz) parallel to the substratum surface are represented by a set of partial differential equations (Eqs. 4-6):

$$\frac{\partial(\hat{\mathbf{u}})}{\partial t} = \varepsilon(t) \cdot \frac{\partial(\hat{\mathbf{j}}_{\mathbf{u}})}{\partial z} - \mathbf{r}_f \quad (4)$$

$$\frac{\partial(\hat{\mathbf{x}}_a)}{\partial t} = \varepsilon(t) \cdot \frac{\partial(\hat{\mathbf{j}}_{\mathbf{x}_a})}{\partial z} + Y_{x/\hat{\mathbf{u}}} \cdot \mathbf{r}_{\hat{\mathbf{u}}} \left(1 - \frac{\Delta c}{\hat{\mathbf{x}}_a R_c} \right) - (b_x + \hat{\lambda}_a) \cdot \hat{\mathbf{x}}_{af} \quad (5)$$

$$\frac{\partial(\hat{\mathbf{x}}_f)}{\partial t} = \varepsilon(t) \cdot \frac{\partial(\hat{\mathbf{j}}_{\mathbf{x}_f})}{\partial z} + Y_{x/\hat{\mathbf{u}}} \cdot \mathbf{r}_{\hat{\mathbf{u}}} \frac{\Delta c}{\hat{\mathbf{x}}_a R_c} + (1 - f_d) \cdot b_x \cdot \hat{\mathbf{x}}_{af} - \hat{\lambda}_i \cdot X_{if} \quad (6)$$

(Molokwane, 2010), where $\hat{\mathbf{j}}_{\mathbf{u}} = D_{\mathbf{u}\hat{\mathbf{u}}} \partial \hat{\mathbf{u}}/\partial z$, mass flux term for dissolved species (ML^2T^{-1}), $\hat{\mathbf{j}}_{\mathbf{x}} = D_{\mathbf{x}\hat{\mathbf{x}}} \partial \hat{\mathbf{x}}/\partial z$, mass flux of biomass (ML^2T^{-1}), $\Delta c = (C_{z_n+\Delta z} - C_{z_n})$, is the change in Cr(VI) concentration across an infinitesimal section (δz), $C = C_{z_n}$, Cr(VI) concentration at a location z_n , $C_{z_n+\Delta z}$ = Cr(VI) concentration at an incremental location $z_n+\Delta z$ towards the liquid/biofilm boundary, $R_c = \text{Cr(VI) reduction capacity of } E. coli \text{ cells (g Cr(VI) per g cells)}$, ε = is a biofilm porosity constant ($V_{\text{voids}}/V_{\text{total}}$), f_d = biodegradable fraction of biomass. Vector quantities are given as: $b_x = \{ b_{xp}, b_{xE} \}$, cell death rate coefficient (T^{-1}); $\hat{\lambda}_a = \{ \hat{\lambda}_{ap}, \hat{\lambda}_{aE} \}$, viable cell detachment rate coefficients (T^{-1}), and $Y_{x/\hat{\mathbf{u}}} = \{ Y_p, Y_E \}$, is the biomass yield of *P. putida* and *E. coli* (g cells per g carbon source). The reaction term $\mathbf{r}_{\hat{\mathbf{u}}}$ is expanded in the kinetic expressions presented in Eqs. 7-9:

$$\frac{dC}{dt} = \frac{k_{mc} \cdot C \cdot X_E^o}{K_c + C \cdot (1 + O_2/K_{io})} \cdot \left(\frac{1}{1 + (P - P_r)/K_{pe}} - \frac{C_o - C}{X_E^o R_c} \right) \quad (7)$$

$$\frac{dP}{dt} = \frac{k_{mp} \cdot P}{K_p + P + P^2/K_{ip}} \cdot \frac{X_p}{1 + (C - C_r)/K_{cp}} \quad (8)$$

$$\frac{dU}{dt} = + \frac{k_{mu} \cdot U \cdot X_E}{K_u + U} - \frac{1}{Y_u} \left(\frac{k_{mp} P}{K_p + P + P^2/K_{ip}} \cdot \frac{K_{iu}}{K_{iu} + U} \left(\frac{X_p}{1 + (C - C_r)/K_{cp}} \right) \right) \quad (9)$$

for Cr(VI) reduction, phenol degradation and metabolite removal, respectively.

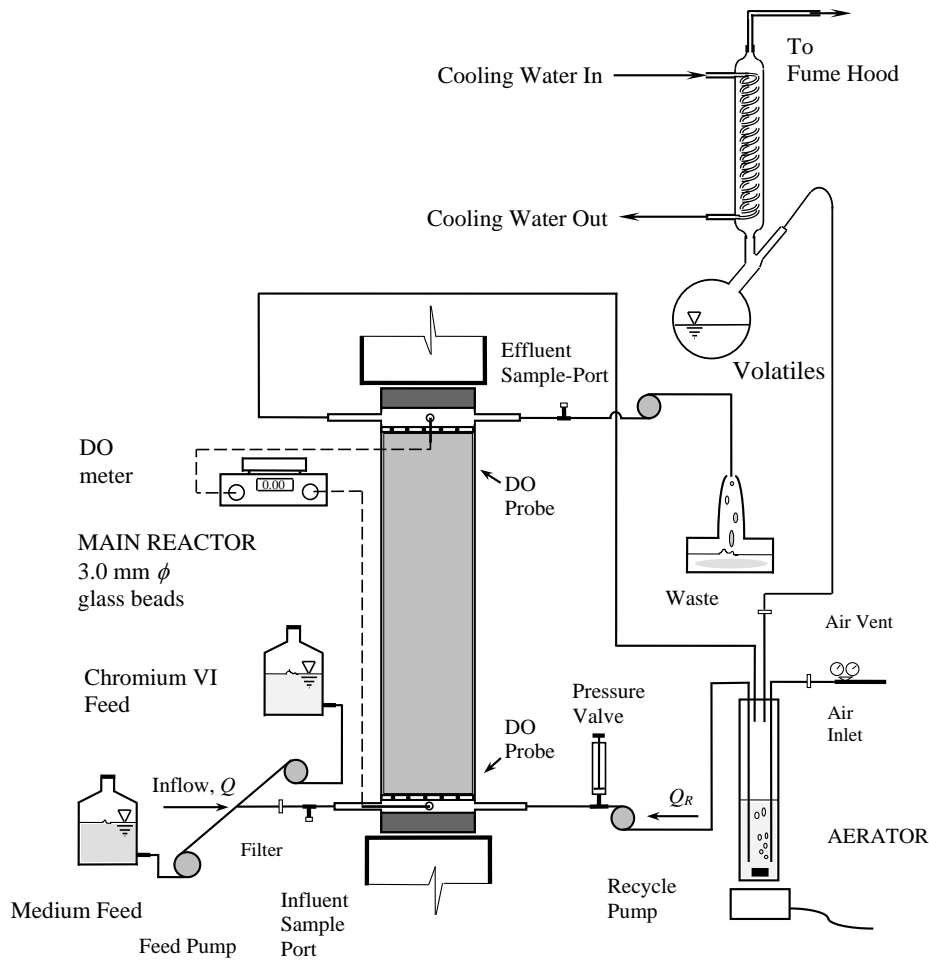


Figure 1: Biofilm reactor configuration.

2.3 Biofilm Reactor Theoretical Basis

The program Sugal 2.1 by Hunter (1995) was interfaced with the simulation program using Modified Sugal GA subroutine (Chirwa, 2001). The Genetic Algorithm uses the fitness function, $f_i(\sigma)$, and an evolutionary search engine to find the best parameters for the system of equations (Eqs. 10-11):

$$RSS = \frac{1}{n - q} \sum_{i=1}^n (y_i^{obs} - y_i^{pred})^2 \quad (10)$$

$$f_i(\sigma) = [RSS]^{-1} \quad (11)$$

where RSS = residual sum of squares, $f_i(\sigma)$ = fitness function, n = number of points to evaluate, q = number of parameters, $\mathbf{y}_i^{\text{pred}}$ = model prediction for a given set of parameters, and $\mathbf{y}_i^{\text{obs}}$ = a corresponding experimental value. The genetic algorithm was terminated with a coarse set of parameters within vicinity of the true optima. A faster converging gradient method, the Levenberg-Marguardt algorithm, was used to fine tune convergence to the global optimum.

3. Results and Discussion

3.1 Elimination of False Optima Using the GSA

In this study, false optima were rejected by determining parameters that yielded a minimum combined MRSS (Eq. 7) and the evolutionary fitness function $f_i(\sigma)$ (Eq. 11) with each parameter expressed as randomized chromosomes in Genetic Search Algorithm (GSA). The response surface model plots Figs. 2 and 3 simulate

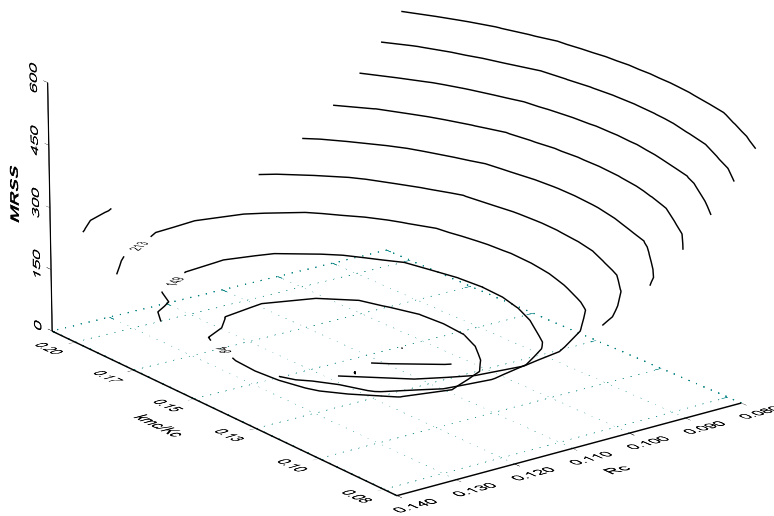


Figure 2: Determination of 'true optima' for the coefficients k_{mc} , K_c and R_c in a biofilm reactor by calculating the minimum residual sum of squares difference (MRSS) using the Genetic Search Algorithm.

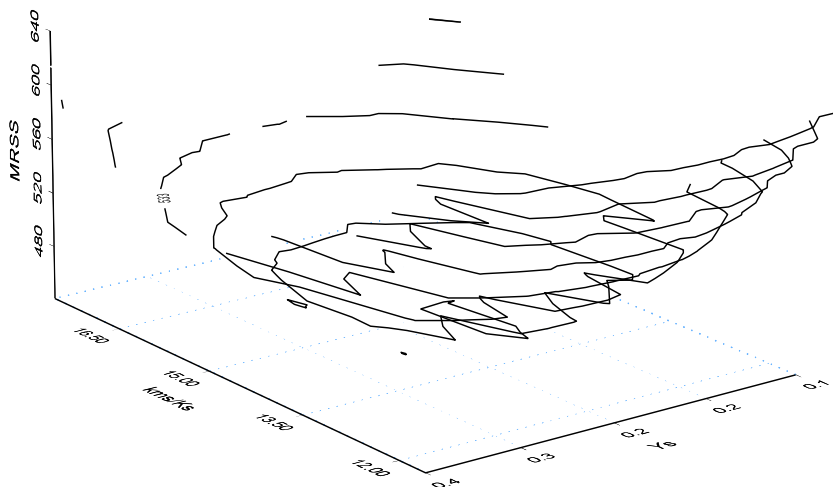


Figure 3: Determination of 'true optima' for the coefficients k_{mc} , K_c and R_c in a biofilm reactor under rough numerical terrain under failure conditions by calculating the minimum residual sum of squares difference (MRSS) using the Genetic Search Algorithm.

the search area for three kinetic parameters for Cr(VI) reduction and phenol degradation which were used to determine global optimum values corresponding to minimum MRSS values were computed in the finite difference search area for Cr(VI) bioconversion rate coefficient k_{md}/K_c vs. R_c and substrate bioconversion rate coefficient k_{ms}/K_s vs. Y_s . The parameters were separated to present the two underlying kinetics, i.e., Cr(VI) reduction and substrate (phenol) utilization. The contours were generated using a 3D contour feature of Axum 5.0 (MathSoft Ware, Cambridge, UK). A contour of 95% confidence passed through $k_{md}/R_c = 0.12$ and 0.16 L/mg cells/d and $R_c = 0.116$ and 0.124 mg Cr(V)/mg cells, and $MRSS = 453$ mg²/L². Parameters were optimised for Cr(VI) reduction rate kinetics in a smooth terrain (Fig. 2), and for phenol degradation rate kinetics from data with wider variations (Fig. 3).

3.2 Final Effluent Cr(VI) Fit Results

Model output concentration plotted with optimized kinetic parameters was plotted against measured data (Fig. 4). The model predicted the trend of the data closely with errors less errors than previous models (Sendin et al., 2004). The model predicted effluent Cr(VI) concentration well with 98.9% confidence ($\sigma_y^2 = 2.37$ mg²/L², $N = 119$) and effluent glucose and phenol concentration with 96.4% and 99.3% confidence ($\sigma_{y(w)}^2 = 5402$ mg²/L², $N = 121$, $w = 100$) over a wide range of Cr(VI) loadings.

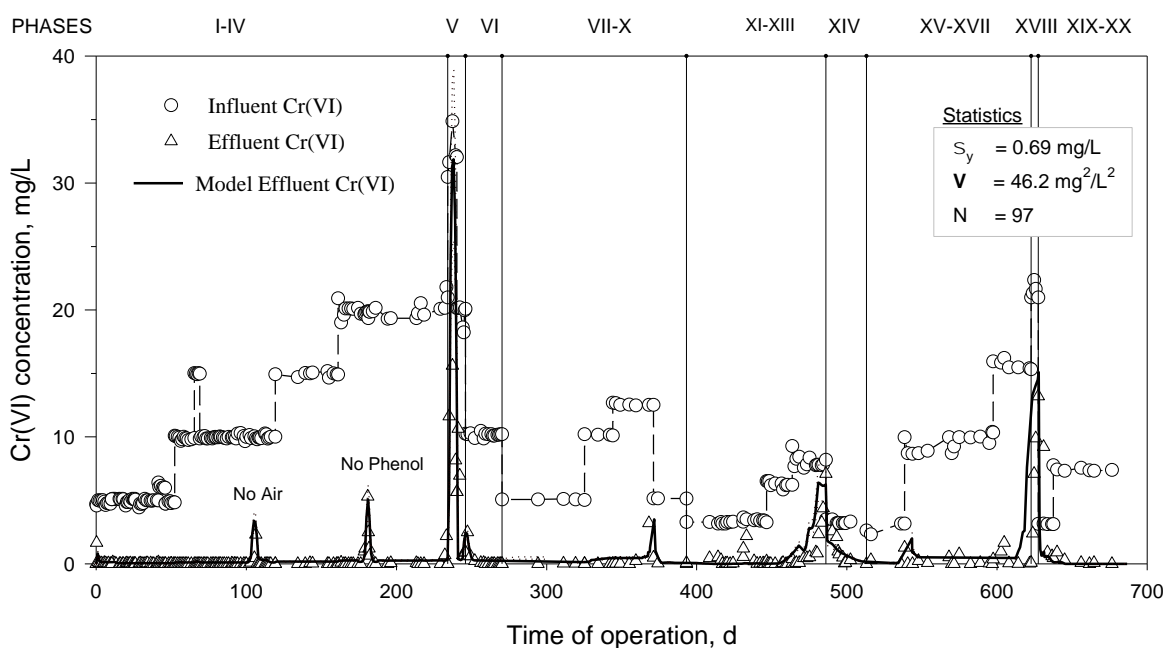


Figure 4. Effluent Cr(VI) concentration performance data and predictive model after parameter optimisation.

3.3 Optimized Kinetic and Physical Parameters

The model predicted well effluent Cr(VI) and phenol concentration with low residual sum of squares between predicted and measured effluent values (Fig. 4, phenol not shown) are presented in Table 1. The variances, $V = 358.1$ ($N = 97$) for Cr(VI) and $V_{(w)} = 1180.5$ ($N = 88$) for phenol (weighing factor $w = 10$), yielded a very low probability for model rejection: $p_{\alpha(0.5)}(0.00086)$ and $p_{\alpha(0.5)}(0.00031) < 0.001$ for Cr(VI) and phenol, respectively. Confidence intervals in Fig. 4 were constructed based on the joint sensitivities of the Cr(VI) reduction parameters k_{mc} , K_c , and R_c , and phenol utilization parameters k_{mp} , K_p , and Y_p using Eqs. 9 and 10. Regression analysis using Pearson's coefficient of correlation showed 98.6% confidence in predicted Cr(VI) and approximately 93.4% confidence in predicted effluent phenol concentration. Error analysis did not include metabolite kinetic parameters due to insufficient metabolites data collected under the transient-state conditions.

4. Conclusions

The model predicted effluent Cr(VI) concentration well with 98.9% confidence ($\sigma_y^2 = 2.37$ mg²/L², $N = 119$) and effluent glucose and phenol concentration with 96.4% and 99.3% confidence ($\sigma_{y(w)}^2 = 5402$ mg²/L², $N = 121$, $w = 100$) over a wide range of Cr(VI) loadings (10–500 mg Cr(VI)/L/d). The results show the potential of predicting real-time performance and determination of scale-up parameters for a complex biofilm reactor system using a robust evolutionary algorithm.

Table 1: The best fitting parameters for the coculture system

Parameter	Value	CV%	Units
a. Optimized parameters			
k_{mc}	0.095	15	1/h
K_c	9.1	8.2	mg/L
R_c	0.13	4.5	mg/mg
k_{mp}	0.104	0.87	1/h
K_p	76.0	7.7	mg/L
b_{xp}	0.014	1.80	1/h
b_{xe}	0.011	1.87	1/h
Y_p	4.3	5.8	mg/mg
k_{mu}	0.035	11	1/h
K_u	25.3	1.4	mg/L
Y_u	0.85	15.2	mg/mg
Y_e	1.15	15.0	mg/mg
b. Operational parameters			
L_w^\dagger	40, 34, 25.4, 38.5	μm
A_f	0.3140	m^2
$Q_{in(1)}$	0.0001047	m^3/d
$Q_R/Q_{in(1)}$	300	m^3/d
V_B	0.0001047	m^3

Acknowledgments

The study was partially funded by the United States Environmental Protection Agency (U.S.EPA) Grant No. Grant 822307-01-0 awarded to Prof Y.T. Wang of University of Kentucky, National Research Foundation (NRF) through Grant No. SRUG2204072544 and Rand Water Company, through Grant No. RW01413/18 awarded to Prof E.M.N. Chirwa.

References

- Chirwa, E.M.N., 2001, Modeling chromium(VI) reduction in pure and coculture biofilm reactors, PhD Thesis, Civil Engineering Department, University of Kentucky, Lexington, Kentucky.
- Dreyer, W., Druet, P.-E., Gajewski, P., Guhlke, C., 2020, Analysis of improved Nernst–Planck–Poisson Models of compressible isothermal electrolytes, *Zeitschrift für Angewandte Mathematik und Physik*, 71, 119.
- de Lichterfelde, A.C.L., ter Heijne, A., Hamelers, H.V.M., Biesheuvel, P.M., Dykstra, J.E., 2019, Theory of Ion and Electron Transport Coupled with Biochemical Conversions in an Electroactive Biofilm, *Physical Review Applied*, 12, 014018.
- Frössling, N. 1938. *Über die Verdunstung fallender Tropfen* (English: About the evaporation of falling droplets). *Gerlands Beiträge zur Geophysik*, 52, 170–216.
- Jaluague, A.F.I., Beltran, A.B., Aviso, K.B., 2023, Integration of machine learning methods for effluent quality prediction in moving bed biofilm reactor system and chlorination wastewater treatment, *Chemical Engineering Transactions*, 106, 697–702.
- Molokwane, P.E., Chirwa, E.M.N., 2009, Microbial culture dynamics and chromium (VI) removal in packed-column microcosm reactors, *Water Science and Technology*, 60, 381–388.
- Molokwane, P.E., 2010, PhD Thesis, Simulation of In Situ Bioremediation of Cr(VI) in Groundwater Aquifer Environments Using a Microbial Culture Barrier, Department of Chemical Engineering, University of Pretoria, Pretoria, South Africa.
- Samson, E., Marchand, J., Snyder, K.A., 2003, Calculation of ionic diffusion coefficients on the basis of migration test results, *Materials and Structures*, 36, 156–165.
- Sendin, O.H., Moles, C.G., Alonso, A.A., Banga, J.R., 2004, Chapter D4 - Multi-Objective Integrated Design and Control using Stochastic Global Optimization Methods, *Computer Aided Chemical Engineering*, 17, 2004, 555–581.
- Tsai, C.F., Bowwerman, C.G., Tait, J.I., 1996, A Intelligent Adaptive System for Improving the Behaviour of Simple Genetic Algorithms. In *EXPERTSYS-96*, October 1996.
- Wanner, O., Gujer, W., 1986, A Multispecies Biofilm Model, *Biotechnology and Bioengineering*, 28, 3, 314-328.
- WHO, 1975, Assessment of carcinogenicity and mutagenicity of chemical compounds. WHO Scientific Group. WHO Technical Report Series, 546, pp. 24.